How to Improve Spermbot Performance

Veronika Magdanz, Mariana Medina-Sánchez, Yan Chen, Maria Guix, and Oliver G. Schmidt*

Spermbots are biocompatible hybrid machines that consist of microtubes which are propelled by single spermatozoa and have promising features for powering nano and microdevices. This article presents three approaches on how to improve the performance of such spermbots. First, 20 µm microtubes produce faster spermbots compared to the previously reported 50 µm long microtubes. Furthermore, biofunctionalization by microcontact printing and surface chemistry of biomolecules on the inner tube surface improve the coupling efficiency between sperm cell and microtube, and the addition of caffeine results in a speed boost of the sperm-driven micromotor.

1. Introduction

Over the last decade, biohybrid approaches for the actuation of objects and performance of robotic tasks on the microscale have become an increasingly important matter of scientific interest.[1] Besides catalytic micromotors,[2–5] which are promising for sensing[6–8] and environmental monitoring,[9–11] biocompatible solutions are sought after especially for challenging biomedical tasks such as drug delivery[12,13] or noninvasive surgery.[14–16] Motile cells are of special interest as microactuators because they have evolved over millions of years to function efficiently on the microscale in viscous media.[1] Bacteria and contractile muscle cells have been harnessed as propulsion sources in many approaches for the development of biohybrid systems that may perform robotic tasks on the microscale in the future.[17–20]

The sperm-flagella driven microbiorobot which we recently demonstrated[21] is the first example of a remotely controlled movement of a spermatozoon, where the cell becomes captured inside a ferromagnetic microtube and its tail propels the tube forward while it is aligned by an external magnetic field. This approach could be of practical relevance, because it not only uses the sperm cell as a physiological power source but also implies the option of delivering a single sperm cell in a controlled way to a desired location. Therefore, this spermbot has promising applications in the field of reproduction biology, medicine, and technology.[22,23]

The motion of the sperm driven microbiorobot (also referred to as spermbot) was previously characterized in dependence on the tube radius, cell penetration inside the microtube and temperature.[21] The separation of the coupled sperm cells on chip by the use of an external magnetic field was also demonstrated. However, it was reported that the speed loss due to the flagella confinement inside the 50 µm long microtubes is very high and results in an average velocity of 10% of the initial cell speed, depending on tube radius and penetration of the cell. Another drawback is the actual coupling process of the sperm cell with the microtube which occurs randomly and therefore results in a relatively low coupling efficiency.

In this article, three methods are described that improve the performance of the spermbot. First, the rolled up microtubes are designed to be shorter in length (20 µm instead of 50 µm long), second, fibronectin (Fn), a protein which can bind to sperm cell membranes, is added on the inside of the microtube to obtain a better coupling between the motile cells and the microtubes. Third, caffeine is added to the solution of moving spermbots, causing a temporary motility boost of the cells. All these methods improve the performance, resulting on both higher speed of the spermbot and higher coupling efficiency between the microtube and the free sperm cells.

2. Results and Discussion

2.1. Short Microtubes Result in Faster Spermbots

The speed of the spermbot is determined by the confinement of the sperm flagellum inside the microtube.[21] This article demonstrates how the spermbot speed is increased by using short 20 µm microtubes. **Figure 1** displays an array of 50 µm microtubes (A) and 20 µm microtubes (B), fabricated via roll-up nanotechnology.[24] The diameter of the microtubes was tuned to be consistently around 7 µm, which offers the possibility to capture bovine spermatozoa.[21] The shorter tube offers the flagellum the possibility to move more freely and take advantage of its full amplitude (Figure 1D), which is restricted in long microtubes (Figure 1C). The full length of a bovine spermatozoon, including its head (10 µm long) and flagellum, is around 60 µm. Therefore, the 20 µm tubes capture only the cell head and a maximum of 10 µm of the shaft of the flagellum; even if the cell has entered the tube completely (see Video S1, Supporting Information, for a 50 µm long spermbot and Video S2, Supporting Information, for a 20 µm long spermbot). In 50 µm spermbots, the flagellum is often confined over a longer

V. Magdanz, Dr. M. Medina-Sánchez, Y. Chen, Dr. M. Guix, Prof. O. G. Schmidt
Institute for Integrative Nanosciences
IFW Dresden
Helmholtzstr. 20, 01069 Dresden, Germany
E-mail: v.magdanz@ifw-dresden.de

DOI: 10.1002/adfm.201500015

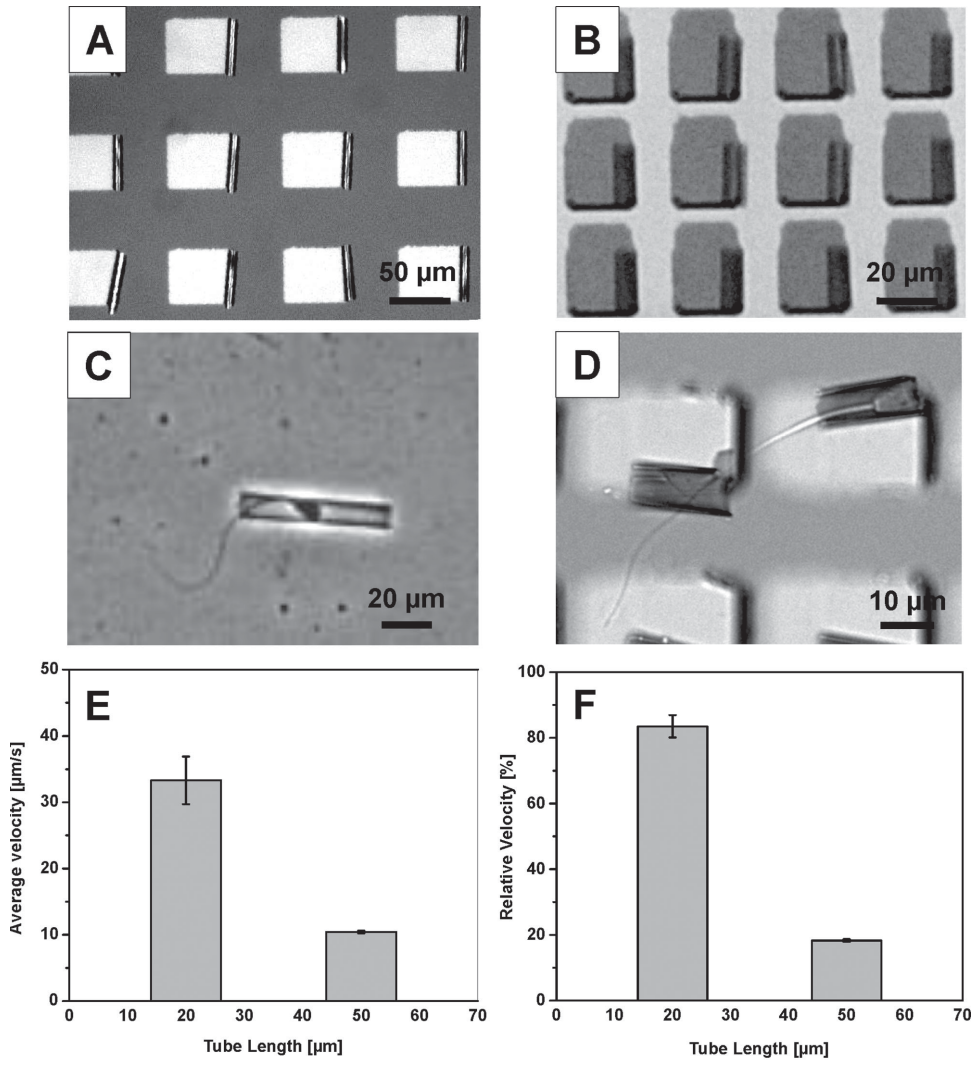

Figure 1. Comparison of spermbot velocity consisting of 50 and 20 µm microtubes. Array of rolled up A) 50 µm and B) 20 µm long microtubes, 7 µm in diameter. A bovine spermatozoon captured inside a C) 50 µm and D) 20 µm rolled up microtube. E) Average and F) relative velocities of the spermbots. The relative velocity is the spermbot velocity divided by the velocity of the free sperm cell times 100. Error bars in E) and F) are values of standard error of the mean.

distance, for example, over 30 µm length of the spermatozoon, as can be seen in Video S1, Supporting Information, and Figure 1C. The average spermbot velocity can be improved from 10.4 µm s^{-1} (in case of a 50 µm long spermbot, standard error of the mean: 0.2 µm s^{-1}) to 33.3 µm s^{-1} (see Figure 1E, standard error of the mean 3.6 µm s^{-1}) with a velocity relative to the initial free cell speed of 83.5% (see Figure 1F, standard error of the mean 3.4%). This means that when microtubes of 20 µm length are used for the cell capture, the initial free cell speed is only reduced by 16.5% compared to an average speed reduction of 81.7% for a 50 µm spermbot. In addition to the flagella confinement, another factor causing the speed reduction in the majority of spermbots is the wobbling of the tube, as it can be observed in Videos S1 and S2, Supporting Information. When the flagellum touches the tube walls, it causes the tube to stagger or even rotate during its forward motion. This effect is likely to contribute to the velocity reduction of spermbots compared to free spermatozoa. The phenomenon and its effect on the spermbot performance are worth being studied in future investigations.

2.2. Biofunctionalization Improves Sperm-Tube Coupling Efficiency

The second method of improving spermbot performance is mainly focused on enhancing the coupling efficiency. In addition to the physical trapping of the cell inside the microtube, the cell-tube binding is supported by attaching biomolecules on the inner tube surface that interact with the sperm cell membrane during the coupling. There are several candidates that are able to bind to sperm cells such as Fn, hyaluronic acid, and others.[25–31] The glycoprotein Fn is a component of the extracellular matrix which is also present in the surroundings of the

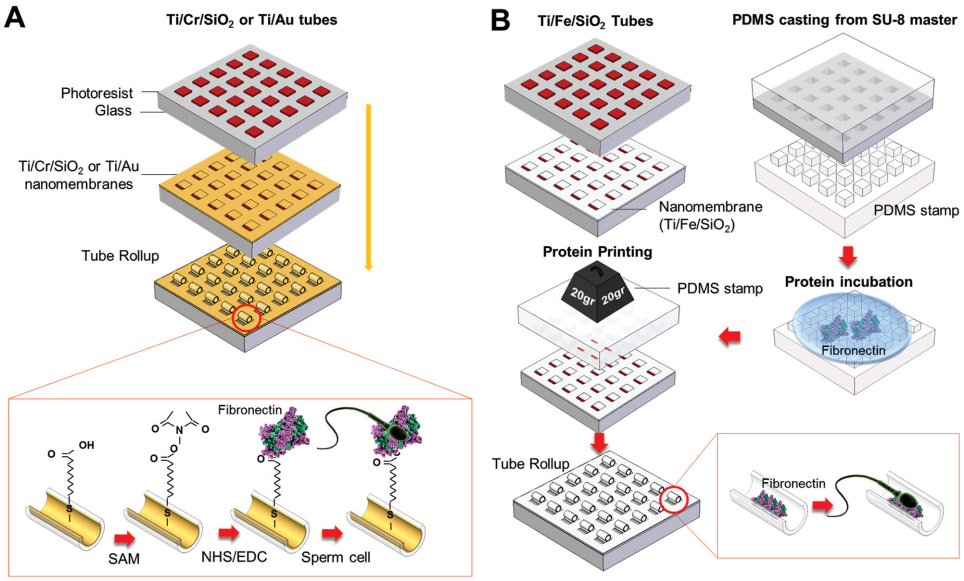

Figure 2. Schematic of two biofunctionalization approaches to immobilize adhesion molecules (proteins such as Fn or carbohydrates such as hyaluronic acid) onto the inner microtube surface. A) By functionalizing a gold or silicon dioxide surface using EDC/NHS (N-(3-Dimethylaminopropyl)-N-ethylcarbodiimide hydrochloride and N-hydroxylsulfosuccinimide) chemistry. The inset in A) shows the formation of a self-assembling monolayer (SAM) onto the gold surface, linking to EDC and NHS and binding of Fn (target protein), then Fn binds to receptors of the sperm cell membrane. B) Microcontact printing onto an array of nanomembranes before roll-up using a PDMS stamp which is casted from an SU-8 master. The stamp is incubated with Fn solution prior to the printing onto the array of deposited nanomembranes. After the printing, the nanomembranes are released into microtubes by solving the sacrificial layer with ethanol. The inset in B) shows the binding scheme of the sperm cell onto the Fn-modified tube.

oocyte.[26] Spermatozoa possess cellular adhesion molecules, also called integrins, on their cell membrane that can bind to Fn. The integrins connect the external environment with the interior cytoskeleton of the cell and act as mediators.[26,27] Fn was recently utilized in a high throughput platform to attach and analyze single spermatozoa to a planar surface.[28] One of the goals in this work was to attach Fn on the inner tube lining. In order to do so, two attachment methods are compared: functionalization of the inner tube surface by surface linker chemistry and microcontact printing technology (see schematics in **Figure 2**).

Hyaluronic acid binds specifically to mature spermatozoa[29–31] and its fluorescently labelled version was used in our experiments for characterization of the two methods of biofunctionalization. Since the molecule contains a fluorescent group, the distribution of the biomolecule on the surface can be directly observed by fluorescent imaging (see **Figure 3**) immediately after functionalization without additional conjugation steps. Hyaluronic acid was also tested as sperm coupling agent inside microtubes, but coupling was not increased as significantly as with Fn.

The initial sample preparation is identical for both methods: a glass substrate patterned with photoresist is prepared by using photolithography. Afterwards, nanomembranes are deposited using electron beam evaporation. The deposition of nanomembranes can be varied to obtain the desired functionalities. Fe introduces a ferromagnetic layer for later external control. Ti offers a good adhesion layer onto the glass substrate and Au or SiO_2 are useful as top layers for surface functionalization, as described in the following paragraph.

For approach A (see Figure 2A) the array of nanomembranes is rolled up into microtubes by etching the underlying photoresist layer using an organic solvent such as ethanol, isopropanol, acetone, or dimethylsiloxane.[24] Functionalization of proteins on the surface of rolled up microtubes has been previously presented.[32–34] In the case of a gold surface as inner tube layer, the first step is the formation of a self-assembling monolayer (SAM) of thiolated molecules ending with carboxylic groups. In case of the silicon dioxide as an active layer for functionalization, the first step is the surface activation by oxygen plasma or piranha treatment and subsequent silanisation with 2% carboxyethylsilantriol, in order to create exposed carboxylic groups. This surface modification creates an anionic, hydrophilic coating. The second step for both surfaces (gold and SiO_2) is the incubation with *N*-(3-Dimethylaminopropyl)-*N*-ethylcarbodiimide hydrochloride (EDC) and *N*-hydroxylsulfosuccinimide (NHS), which activate the carboxylic groups to create a covalent binding with the amino-groups present on the protein (in case of fibronectin) (see Figure 2A). In the case of hyaluronic acid, it is done in the same way, except for the change of the SAM (in the case of gold functionalization), which should have ending amino groups, and in the case of SiO_2, it is necessary to exchange the silane with APTES ((3-aminopropyl)triethoxysilane), which has exposed amino groups that will bind to the carboxylic groups present in the hyaluronic acid in a covalent way. More details can be found in the Experimental Section below.

The second method to attach Fn inside the microtubes is done by microcontact printing. This technique involves the printing of the target protein directly on the nanomembranes before the roll-up of the microtubes. This method is a form of soft-lithography, which was introduced in 1996 by Whitesides and co-workers at Harvard University[35] and was also applied for binding sperm cells onto glass or polystyrene surfaces printed

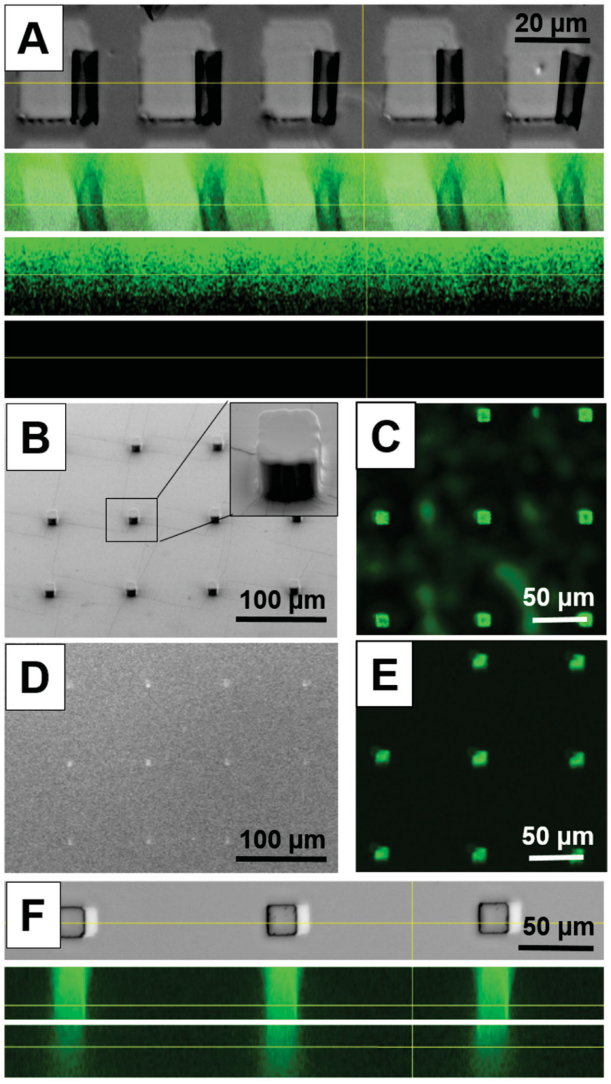

Figure 3. Characterization of the two proposed functionalization strategies. The top image in A) shows 20 µm long microtubes that are functionalized with fluorescent hyaluronic acid using the EDC/NHS chemistry. The second image in A) shows the overlayed DIC (differential interference contrast) and green FITC (fluorescein isothiocyanate) channels in the orthogonal view of the Z-stack. The third image in A) shows only the Z-stack of the FITC channel. The bottom image in A) is the control of nonfunctionalized rolled up microtubes. B) shows the SEM Image of PDMS stamp. C) Fluorescent imaging of the PDMS stamp incubated with fluorescent hyaluronic acid (1 mg mL^{-1} in water). D) SEM (scanning electron microscopy) image of Fn spots printed on a silicon wafer. E) Fluorescent image of fluorescent hyaluronic acid printed on a glass slide after microcontact printing. F) shows nanomembranes before roll-up that have been printed with hyaluronic acid by use of microcontact printing. The second image in F) shows the fluorescent signal of the Z-stack in the FITC channel. The third image in F) shows the control of nonfunctionalized nanomembranes. The weak fluorescent signal comes from the photoresist underneath the nanomembranes. The yellow lines in F mark the position of the orthogonal view.

with Fn.[28] Polydimethylsiloxane (PDMS) stamps with squared pillars (with geometries of 20×20 µm^2 and 50×50 µm^2, height 10 µm) were prepared by using a soft-lithography technique. This PDMS stamp was soaked in a Fn solution, dried with a nitrogen gun and transferred onto the nanomembrane array, achieving an exact alignment with the nanomembrane array (see Figure 2B). After proper alignment, the protein was transferred onto the array by applying a uniform weight onto the stamp (details in the Experimental Section). Subsequently, the nanomembranes were rolled up into tubes by immersing them in ethanol for a few seconds, removing in this way the sacrificial layers underneath the nanomembranes, as it was previously reported by our group.[24]

The two methods have different effects on the local concentration of the protein in the different areas on the tube array. The surface chemistry approach with EDC/NHS attaches the biomolecule on a large area in a uniform manner. Figure 3A shows the fluorescent signal from hyaluronic acid that was functionalized via the EDC/NHS method. It illustrates that the biomolecule is distributed evenly on the glass surface. It is slightly more concentrated where the microtubes are located, as can be seen in the orthogonal view of the Z stack in Figure 3A. Microcontact printing leads to a high quality deposition of the biomolecule in a localized and patterned way.[36,37] During this technique, the target molecule attaches via surface adhesion on the silicon dioxide surface. The scanning electron microscopic image of the PDMS stamp in Figure 3B displays the shape of the pillars that are used to stamp the target molecule onto the substrate. The defined fluorescent signal by the pillars of the PDMS stamp which was soaked in fluorescent hyaluronic acid is displayed in Figure 3C. As shown in Figure 3D–F in the scanning electron and fluorescent images, the printed hyaluronic acid is only present where the stamp pillars were touching the substrate. The bottom image in Figure 3F shows the control image of an array with nonprinted nanomembranes. This proves that the photoresist shows autofluorescence,[38] which causes a weak fluorescent signal in the control image.

After the surface functionalization with Fn or hyaluronic acid by the use of these two techniques, finally, the bovine sperm cells are incubated on the sample containing at least 500 modified microtubes, during 30 min at 37 °C and 5% CO_2. Immediately after incubation, the coupling efficiency was evaluated by microscopic analysis based on the number of microtubes containing spermatozoa in relation to the total number of microtubes.

Hyaluronic acid was tested in 20 µm microtubes and improved the coupling from 1.1% to 3.1% (standard error of the mean: 0.8%). The lower coupling increase of hyaluronic acid compared to Fn (average 4.8%, with standard error of the mean 1.6%, see **Table 1**) can be explained by the specific binding of only matured spermatozoa to hyaluronic acid. It is known that hyaluronic acid is a natural component of the extracellular matrix of the cumulus cells which surround the egg cell and that it is involved in the selection process of spermatozoa prior to fertilization in vivo. Only spermatozoa that have undergone the necessary maturation steps for fertilization named capacitation (i.e., formation of zona pellucida binding sites) and are still viable, contain high DNA integrity, and have not yet acrosome reacted are able to bind to hyaluronic acid.[29–31] The percentage of capacitated cells in a population of spermatozoa is generally around 10% which explains why the increase in coupling success rate is fairly low.[39]

Table 1. Summary of results from functionalization of microtubes via surface chemistry and microcontact printing and its effect on the coupling efficiency between sperm cells and microtubes.

		50 µm tubes	20 µm tubes	Method of biomolecule attachment
Average speed[a)]		10.4 ± 0.2 µm s^{-1}[b)]	33.3 ± 3.6 µm s^{-1}	
Relative speed[c)]		18.3 ± 0.4%[b)]	83.5 ± 3.4%	
Coupling success	Bare microtubes[d)] (control)	23.6 ± 1.9%	1.1 ± 0.2%	...
	+Fn on Au or SiO_2[e)]	38.6 ± 3.6%	4.8 ± 1.6%	Surface chemistry (EDC/NHS linkers)
	+HA on SiO_2[e)]		3.1 ± 0.8%	Surface chemistry (EDC/NHS linkers)
	+µCP Fn on SiO_2[e)]	58.7 ± 2.2%	8.0 ± 1.7%	Adsorption from stamp

[a)]Number of experiments > 12; [b)]Speed data for 50 µm spermbots were taken from type A spermbots (see ref.[21]); [c)]Relative speed of spermbot refers to initial free cell speed of spermatozoon; [d)]In the control samples, microtubes were used that have not been functionalized. Average value from 5 experiments; [e)]Each experiment was conducted 2–3 times with cell count of >100 each time. Notes: Fn: fibronectin, µCP: microcontact printing, EDC: N-(3-Dimethylaminopropyl)-N-ethylcarbodiimide hydrochloride, NHS: N-hydroxylsulfosuccinimide. Standard deviation is displayed as standard error of the mean.

In our study we focus on the use of Fn as sperm binding agent for improving coupling efficiency, because it addresses the general population of sperm cells. Every sperm cell independent of its maturation state is expected to exhibit active Fn binding receptors on its surface. **Figure 4** shows that for Fn-containing 20 µm microtubes the coupling efficiency was improved from 1.1% (control, nonfunctionalized, standard error of the mean 0.2%) to 4.8% by surface chemistry (standard error of the mean 1.6%) and to 8.0% by µCP (microcontact printing) (standard error of the mean 1.7%). In 50 µm microtubes, the coupling efficiency is improved from 23.6% (control, nonfunctionalized tubes, standard error of the mean 1.9%) to 38.6% by surface chemistry with a standard error of the mean of 3.6% and to 58.7% by the µCP method (standard error of the mean: 2.2%). In general, the coupling of spermatozoa inside microtubes occurs solely due to mechanical trapping of the cell inside the tube in case of the nonfunctionalized microtubes. Both methods, µCP and EDC/NHS surface chemistry, improve the coupling efficiency by adding a binding component on the inner tube surface. Microcontact printing results in a better coupling efficiency compared to NHS/EDC chemistry, because it deposits a large amount of target molecule exactly on the nanomembranes before roll-up. Thereby, the local concentration of target molecules is significantly higher inside the tube resulting in a higher number of binding events of spermatozoa inside the microtube. The EDC/NHS method functionalizes the whole array but does not offer a pre-concentration of the target molecule inside the microtube. However, it also causes an increased number of coupling events due to the biochemical linking of the target molecule Fn on the inside of the tube which binds the spermatozoa.

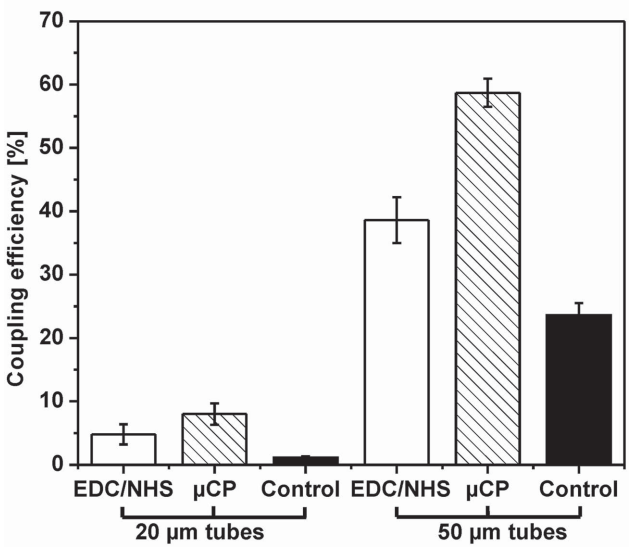

Figure 4. Coupling efficiency of microtubes with bovine sperm cells in 20 and 50 µm microtubes using two different approaches. EDC/NHS: functionalization of Au or SiO_2 surface using surface chemistry or µCP: microcontact printing of the protein directly on the SiO_2 surface. The control samples are microtubes that have not been functionalized.

The coupling efficiency in 50 µm microtubes is generally higher, which can be justified by the stronger confinement effect on the sperm flagellum in 50 µm tubes. The short tail confinement in 20 µm microtubes was mentioned earlier as a reason for higher spermbot velocity, being also the reason for lower coupling success in 20 µm microtubes. This can be illustrated by comparing the sperm cell inside the tube to rotating a rope in circular and wavy motion through a tube. The rope keeps hitting the inner walls of the tube and this causes an impact force on the rope. This impact force is stronger, the longer the tube is. As can be seen in Video S1, Supporting Information, the inner tube area that interacts with the flagellum in a 50 µm long spermbot is larger than in Video S2, Supporting Information, which shows a 20 µm long spermbot. Therefore, in a 20 µm tube it is easier for the spermatozoa to slip through because the impact force on the flagellum which is thought to cause the trapping is much lower than in a 50 µm long tube. The influence of tube radius can be neglected because both, 20 µm and 50 µm microtubes, were fabricated to have a diameter of around 7 µm.

2.3. Caffeine Addition for a Spermbot Speed Boost

The last approach to improve spermbot performance is carried out by adding caffeine to the sperm medium. Caffeine is a phosphodiesterase inhibitor that increases spermatozoon motility.[40] As an important step in achieving fertilization, caffeine is used for the induction of in vitro acrosome reaction in mammalian sperm cells.[41] It is also known that caffeine

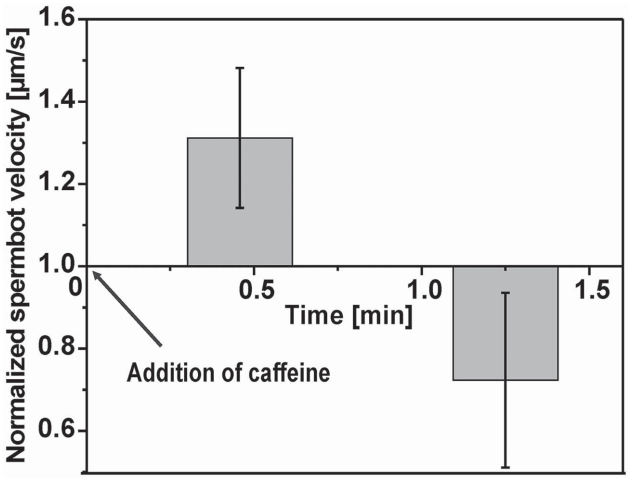

Figure 5. Spermbot speed boost by addition of 2×10^{-3} M caffeine to the medium. The graph shows the normalized spermbot speed (in relation to initial spermbot speed before the caffeine addition) over time. Total number of 29 cases.

increases sperm motility by causing hyperactivity. Thereby, caffeine increases calcium levels in the cell by opening calcium channels in the plasma membrane of the sperm flagellum. The raised calcium level causes hyperactivation which is characterized by an asymmetric flagella beating and enables the cell to penetrate the cumulus cells and the zona pellucida which surround the egg cell. This indicates that hyperactivation helps sperm to reach the oocyte and fertilize it.[42,43]

With the aim of increasing sperm cell motility once the cell is captured inside the microtube and functions as a spermbot, 1 µL of 100×10^{-3} M solution of caffeine in SP-TALP (modified Tyrode's albumin lactate pyruvate medium) was added to a solution of 50 µL actively swimming spermbots. The spermbots were video-recorded and the velocity was calculated over time. **Figure 5** illustrates that the spermbot velocity is increased slightly about half a minute after addition of caffeine to the medium (to a final concentration of 2×10^{-3} M).[44]

Unfortunately, this increase in motility by caffeine is only temporary and results in a lower velocity after about 1.25 min. However, caffeine leads to a temporary speed boost of the spermbot and increases their speed by 30% on average. It is known from studies about the influence of caffeine on spermatozoa, that this might be a transitory effect and that the speed boost diminishes over time.[45,46] The biochemical response to caffeine is not equal in each cell. Depending on the initial cell state and cytoplasmic calcium concentration before caffeine addition, the caffeine addition might increase the velocity more or less.[44] In addition, the experimental setup did not always allow a precise velocity change analysis over a short time. Sometimes it was difficult to track the spermbot during and after the caffeine addition. These reasons result in the large error bars in Figure 5.

3. Conclusion

In conclusion, three approaches are presented to improve spermbot performance: shorter microtube design for higher spermbot speed, binding of sperm cells on fibronectin-functionalized tube surface for better coupling efficiency and speed boosting by addition of caffeine. These versatile approaches demonstrate that the performance of spermbots can be influenced by many different factors, such as physical confinement of the single cell and interaction with biomolecules.

The two approaches to attach biomolecules to the inner tubes surfaces via surface chemistry and microcontact printing both improve the trapping of sperm cells inside the microtubes. In nonfunctionalized microtubes, the trapping happens solely due to physical confinement. Here, the sperm membrane-Fn binding increases the number of coupling events attributable to biochemical interaction of the receptors located in the sperm cell membrane and the Fn that is attached on the inner tube surface. The microcontact printing method results in a high quality deposition method for localized biomolecule immobilization on the nanomembranes compared to the surface functionalization by EDC/NHS chemistry. We demonstrate that microcontact printing can be combined with rolled up nanotech in order to print biomolecules or other target molecules in specific spots on the nanomembranes. One huge advantage of the microcontact printing method is that it circumvents the need of linker agents and that it can be applied before the roll-up of nanomembranes. Still, surface chemistry is a good option for creating a uniform distribution of target molecules on a larger surface.

With the presented methods we achieve an increase of the average spermbot velocity to 33.3 µm s^{-1} for 20 µm long microtubes and an increase of coupling efficiency to 58.7% for 50 µm microtubes. Table 1 gives a summary of the achieved results. Even if this article describes substantial improvements in spermbot performance, the spermbot design could be enhanced further to optimize sperm cell motion inside the trapping microstructure. Furthermore, the coupling still relies on random events and is not controlled. It will be helpful to develop a method that attaches previously selected single sperm cells to the microtubes in a controlled manner. Overall, it will be helpful for future applications to gain a deeper understanding of the interaction between sperm cells and their trapping inside microtubes.

4. Experimental Section

Fabrication of Microtubes: Photomasks with 50 × 50 µm squares and 20 × 20 µm squares were written using the laser lithographic mask writing tool DWL66. 18 × 18 mm cover glasses were spin-coated with photoresist ARP 3510, prebaked and patterned with the 50 µm or 20 µm square photomask by photolithography. The photoresist was developed subsequent to the lithographic step. Electron beam evaporation was conducted with an Edwards AUTO500. The parameters for the 70° angled deposition were: 10 nm Ti at 3 A s^{-1}, 10 nm Cr at 1 A s^{-1} and as last layer either 5 nm SiO_2 or 10 nm Au. The nanomembranes were rolled up by removal of the photoresist underneath the nanomembranes by addition of ethanol (70%). This resulted in 20 or 50 µm long microtubes, respectively, with a diameter of 6–7 µm.

Microcontact Printing: The microcontact printing was done on the array of nanomembranes before their rollup. Polydimethylsiloxane (PDMS) stamps with squared pillars (with geometries of 20 × 20 μm^2 and 50 × 50 μm^2, height 10 µm) were prepared by using soft-lithography technique. Briefly, a SU8 master was fabricated by standard

photolithography methods. Then the PDMS (Sylgrad 184, Dow Corning, Germany) prepolymer was mixed with the curing agent at a ratio of 10:1 (w/w) and degassed by using a desiccator. Then the PDMS was poured onto the SU8 master and baked overnight at 65 °C. Afterwards, this PDMS stamp was soaked in a fibronectin solution (1 mg mL^{-1}) or fluorescein hyaluronic acid (1 mg mL^{-1}) for 40 min, dried with a nitrogen gun and transferred onto the nanomembrane array using the lambda aligner (FINEPLACER lambda, USA), achieving an exact alignment with the nanomembrane array (see Figures 2B and 3A). After proper alignment, the biomolecule was transferred on the array by applying an uniform weight (20 gr) onto the stamp, during 40 min. Afterwards, the nanomembranes were rolled up into tubes by immersing them in ethanol, removing in this way the sacrificial layers behind the nanomembranes, as it was reported previously for our group.[24]

Functionalization of Rolled Up Microtubes: The array of rolled up microtubes was chemically activated with a piranha treatment (25% H_2SO_4 and 15% H_2O_2 for 1 h) immediately after rollup in ethanol. Afterwards, the sample was washed in water. For the silanization, 2% carboxytheylsilantriol was placed on the sample and incubated for 3–4 h at 37 °C. In case of fluorescein hyaluronic acid functionalization, 2% APTES was incubated for 1–2 h on the substrate with rolled up microtubes. The samples were washed three times with water and then immersed in *N*-(3-Dimethylaminopropyl)-*N*-ethylcarbodiimide hydrochloride (EDC) and *N*-hydroxylsulfosuccinimide solution (NHS) in a 1:1 mixture with a final concentration of 0.1 M EDC and 0.025 M NHS) and 20 µL of Fn (1 mg mL^{-1}) or fluorescein hyaluronic acid (1 mg mL^{-1}), respectively. The sample was incubated overnight at room temperature and afterwards washed three times in water.

Sperm Treatment: Cryopreserved bovine semen straws (a kind donation from Masterrind GmbH) were thawed at 37 °C for 5–10 min and resuspended in 3 mL SP-TALP medium (modified Tyrode's Albumin Lactate Pyruvate Medium) and incubated for 10 min at 37 °C. The array of microtubes was immersed in the sperm cell solution and incubated for 30 min at 37 °C. Afterwards, the array was analyzed by optical microscopy and the cell-tube coupling events were counted. For each set of experiment of functionalization, 2–3 repetitions were done and 100–1000 microtubes were analyzed each time regarding the coupling with sperm cells. All chemicals were obtained from Sigma-Aldrich (Germany), except for SP-TALP (Caisson Laboratories, USA).

Imaging and Analysis: Optical microscopy was carried out with the inverted Zeiss Observer A.1. Videos were recorded using the Miro eX2 high speed camera from Vision Research and the Phantom Camera software. Fluorescent images were taken with the Cellobserver in differential interference contrast channel and GFP channel. For the Z-stacks, a distance of 0.5 µm between each image was used. Velocity calculation was done by tracking in ImageJ (image analysis software available free of charge). ImageJ was also used to obtain orthogonal views of the Z-stacks on images and the brightness and contrast values were adjusted to equal minimum and maximum values in order to compare the fluorescent signal qualitatively.

Supporting Information

Supporting Information is available from the Wiley Online Library or from the author.

Acknowledgements

The authors thank Masterrind GmbH for kind donation of cryopreserved bovine semen. We thank Dr. S. Harazim and Sandra Nestler for clean room support, B. Eichler for AFM measurements, Dr. D. Makarov, A. Kutscher, and D. Karnaushenko for support in initial trials with microdrop deposition technique. V. Magdanz thanks L. Helbig for support during functionalization procedures and B. Koch for assistance with fluorescent imaging. We thank the German Science Foundation (DFG) for the funding through the priority program SPP1726 "Microswimmers: From single particle motion to collective behaviour" and the Volkswagen Foundation (86 362).

Received: January 2, 2015
Revised: February 20, 2015
Published online: March 26, 2015

[1] R. W. Carlsen, M. Sitti, *Small* **2014**, *10*, 3831.
[2] R. F. Ismagilov, A. Schwartz, N. Bowden, G. M. Whitesides, *Angew. Chemie Int. Ed.* **2002**, *41*, 652.
[3] W. F. Paxton, K. C. Kistler, C. C. Olmeda, A. Sen, S. K. St. Angelo, Y. Cao, T. E. Mallouk, P. E. Lammert, V. H. Crespi, *J. Am. Chem. Soc.* **2004**, *126*, 13424.
[4] A. A. Solovev, Y. F. Mei, E. Bermúdez Ureña, G. S. Huang, O. G. Schmidt, *Small* **2009**, *5*, 1688.
[5] W. Gao, S. Sattayasamitsathit, J. Orozco, J. Wang, *J. Am. Chem. Soc.* **2011**, *133*, 11862.
[6] D. Kagan, P. Calvo-Marzal, S. Balasubramanian, S. Sattayasamitsathit, K. M. Manesh, G. U. Flechsig, J. Wang, *J. Am. Chem. Soc.* **2009**, *131*, 12082.
[7] J. Wu, S. Balasubramanian, D. Kagan, K. M. Manesh, S. Campuzano, J. Wang, *Nat. Commun.* **2010**, *1*, 36.
[8] J. Simmchen, A. Baeza, D. Ruiz, M. J. Esplandiu, M. Vallet-Regí, *Small* **2012**, *8*, 2053.
[9] M. Guix, J. Orozco, M. Garcia, W. Gao, S. Sattayasamitsathit, A. Merkoci, A. Escarpa, J. Wang, *ACS Nano* **2012**, *6*, 4445.
[10] L. Soler, V. Magdanz, V. M. Fomin, S. Sanchez, O. G. Schmidt, *ACS Nano* **2013**, *7*, 9611.
[11] J. Orozco, V. Garcia-Gradilla, M. D'Agostino, W. Gao, A. Cortes, J. Wang, *ACS Nano* **2013**, *7*, 818.
[12] W. Gao, D. Kagan, O. S. Pak, C. Clawson, S. Campuzano, E. Chuluun-Erdene, E. Shipton, E. E. Fullerton, L. Zhang, E. Lauga, J. Wang, *Small* **2012**, *8*, 460.
[13] R. Mhanna, F. Qiu, L. Zhang, Y. Ding, K. Sugihara, M. Zenobi-Wong, B. J. Nelson, *Small* **2014**, *10*, 1953.
[14] T. G. Leong, C. L. Randall, B. R. Benson, N. Bassik, G. M. Stern, D. H. Gracias, *Proc. Natl. Acad. Sci. USA* **2008**, *106*, 703.
[15] A. A. Solovev, W. Xi, D. H. Gracias, S. M. Harazim, S. M. Deneke, S. Sanchez, O. G. Schmidt, *ACS Nano* **2012**, *6*, 1751.
[16] W. Xi, A. A. Solovev, A. N. Ananth, D. H. Gracias, S. Sanchez, O. G. Schmidt, *Nanoscale* **2013**, *5*, 1294.
[17] R. K. Soong, G. D. Bachand, H. P. Neves, A. G. Olkhovets, H. G. Craighead, C. D. Montemagno, *Science* **2000**, *290*, 1555.
[18] S. Martel, C. C. Tremblay, S. Ngakeng, G. Langlois, *Appl. Phys. Lett.* **2006**, *89*, 233904.
[19] B. Behkam, M. Sitti, *Appl. Phys. Lett.* **2007**, *90*, 023902.
[20] B. J. Williams, S. V. Anand, J. Rajagopalan, M. T. A. Saif, *Nat. Commun.* **2014**, *5*, 3081.
[21] V. Magdanz, S. Sanchez, O. G. Schmidt, *Adv. Mater.* **2013**, *25*, 6581.
[22] V. Magdanz, O. G. Schmidt, *Expert Opin. Drug Deliv.* **2014**, *11*, 1125.
[23] V. Magdanz, M. Guix, O. G. Schmidt, *Robot. Biomimetics* **2014**, *1*, 1.
[24] Y. F. Mei, G. S. Huang, A. A. Solovev, E. Bermudez Urena, I. Moench, F. Ding, T. Reindl, R. K. Y. Fu, P. K. Chu, O. G. Schmidt, *Adv. Mater.* **2008**, *20*, 4085.
[25] P. Bansal, S. K. Gupta, *Indian J. Mad. Res.* **2009**, *130*, 37.
[26] E. S. Diaz, M. Kong, P. Morales, *Hum. Reprod.* **2007**, *22*, 1420.
[27] G. Wennemuth, P. J. Schiemann, W. Krause, A. M. Gressner, G. Aumüller, *Int. J. Androl.* **1997**, *20*, 10.
[28] J.-P. Frimat, M. Bronkhorst, B. de Wagenaar, J. G. Bomer, F. Van der Heijden, A. Van den Berg, L. I. Segerink, *Lab Chip* **2014**, *14*, 2635.

[29] G. Huszar, C. C. Ozenci, S. Cayli, Z. Zavaczki, E. Hansch, L. Vigue, *Fertil. Steril.* **2003**, *79*, 1616.
[30] A. Yagci, W. Murk, J. Stronk, G. Huszar, *J. Andrology* **2010**, *31*, 566.
[31] L. Parmegiani, G. E. Cognigni, S. Bernardi, E. Troilo, S. Taraborrelli, A. Amone, A. M. Maccarini, M. Filicori, *Fertil. Steril.* **2012**, *98*, 632.
[32] S. Sanchez, A. A. Solovev, Y. Mei, O. G. Schmidt, *J. Am. Chem. Soc.* **2010**, *132*, 13144.
[33] W. Xi, C. K. Schmidt, S. Sanchez, D. H. Gracias, R. E. Carazo-Salas, S. P. Jackson, O. G. Schmidt, *Nano Lett.* **2014**, *14*, 4197.
[34] B. Koch, S. Sanchez, C. K. Schmidt, A. Swiersy, S. P. Jackson, O. G. Schmidt, *Adv. Healthc. Mater.* **2014**, *3*, 1932.
[35] J. L Wilbur, A. Kumar, H. A Biebuyck, E. Kim, G. M Whitesides, *Nanotechnology* **1996**, *7*, 452.
[36] H. D. Inerowicz, S. Howell, F. E. Regnier, R. Reifenberger, *Langmuir* **2002**, *18*, 5263.
[37] U. S. Schwarz, C. M. Nelson, P. Silberzan, *Soft Matter* **2014**, *10*, 2337.
[38] J.-H. Pai, Y. Wang, G. To'A Salazar, C. E. Sims, M. Bachman, G. P. Li, N. L. Allbritton, *Anal. Chem.* **2007**, *79*, 8774.
[39] M. Eisenbach, L. C. Giojalas, *Nat. Rev.* **2006**, *7*, 276.
[40] J. Barkay, H. Zuckerman, D. Sklan, S. Gordon, *Fertil. Steril.* **1977**, *28*, 175.
[41] N. Nabavi, F. Todehdehghan, A. Shiravi, *Iran J. Reprod. Med.* **2013**, *11*, 741.
[42] S. S. Suarez, A. A. Pacey, *Hum. Reprod. Update* **2006**, *12*, 23.
[43] P. Jones, W. Gottlieb, S. S. Suarez, *Am. Bio. Teach.* **2007**, *69*, e81.
[44] H.-C. Ho, S. S. Suarez, *Biol. Reprod.* **2001**, *65*, 1606.
[45] A. I. Traub, J. C. Earnshaw, P. D. Brannigan, W. Thompson, *Fertil. Steril.* **1982**, *37*, 436.
[46] M. T. Mbizvo, R. C. Johnston, G. H. W. Baker, *Fertil. Steril.* **1993**, *59*, 1112.